Title
The Direct and Indirect Effects of HIV-1 on Cells of the Central Nervous System

Author
Durrani, Amina

Publication Date
2022-06-03

Undergraduate

The Direct and Indirect Effects of HIV-1 on Cells of the Central Nervous System

Amina Durrani
MIMG 199 Winter 2022

Abstract:
HIV-1 is the most common Human Immunodeficiency Virus. It attacks the body's immune system and kills CD4 cells. Antiretroviral therapies (ART) have been developed to combat HIV-1, however HIV-1 persistsis due to reservoirs of latent virus in the body. In addition, up to 50% of patients on ART will develop motor/memory impairments later in life with HIV-1 associated neurocognitive diseases (HAND) (Rai 2020). Previous experiments have found that cells in the central nervous system (CNS), such as astrocytes and microglia, are potential reservoirs for latent HIV in the body and could contribute to HAND (Wallet 2019). However, the results are conflicting as to which cell types can be infected. Targeting these reservoirs in vivo is challenging due to the blood-brain barrier preventing drugs from reaching these reservoirs (Wallet 2019). In the lab, the mechanisms of HIV infection can be studied using the replication competent strain, AD8 or dEnv, a virus pseudotyped with an envelope from Vesicular Stomatitis Virus (VSV) that has a different entry mechanism to infect cells, but cannot replicate (Hastie 2013). In my research project, I hypothesize that AD8 will selectively infect microglial cells. Microglial cells infected with either AD8 or dEnv will then lead to reactive changes in astrocytes and neurons leading to the pathology seen in HAND. In this study, the production of human pluripotent stem cell (hPSC) derived microglia, neurons, and astrocytes was optimized using immunohistochemistry (IHC) and qPCR. The effects of HIV infection on microglia proliferation and migration was determined. After successfuL differentiation of neural progenitor cells (NPCs) to neurons and astrocytes, a tri-culture system was then optimized to study the indirect effects of HIV infection, via the consequence of infected microglia on other cells in the CNS.

Introduction:

Approximately 40 million people around the world have been infected by Human Immunodeficiency Virus (http://www.cdc.gov/hiv/library/reports/hiv-surveillance.html 2021). HIV-1 is the most common Human Immunodeficiency Virus and it infects cells by competitively binding the host CD4 T cell receptor and CXC4 or CCR5 coreceptors. HIV-1 hijacks the CD4 T cell machinery in order to replicate itself and destroys CD4 T cells in the process. CD4 T cells are essential to the host adaptive immune response because they direct B cell antibody production and generate cytotoxic and memory CD8 T cells to fight subsequent viral infections (Swain 2012).

There is no cure for HIV, but combined antiretroviral therapies (cART) have been used as a treatment for HIV-1 infection, reducing it to a chronic infection instead of a fatal one. However, cART is not completely successful. If treatment is stopped, HIV-1 levels return due to the reservoirs of latent HIV-1 in microglia and macrophages. In addition, 20-50% of patients will go on to develop HIV-associated neurocognitive disorders (HAND) (Rai 2020). HAND is comprised of three main disorders: asymptomatic neurocognitive impairment, mild neurocognitive disorder, and HIV-associated dementia. Current treatments for HAND are focused on removing the latent reservoirs of infected cells through (1) the shock and kill strategy, (2) block and lock method, (3) stem cell transplantation using genome editing to remove the co-receptor CCR5, and (4) using CRISPR-Cas9 to remove integrated HIV. The shock and kill strategy reactivates latent HIV using latency reversing agents and then tries to kill these infected cells via cART. On the other hand, the block and lock method utilizes latency promoting agents and cART to promote latency and prevent cells from becoming HIV-active.

The stem cell transplantation approach involves editing the genome to knockdown the coreceptor CCR5 of bone marrow-derived stem cells before transplantation into a patient. The CRISPR/Cas9 system works to remove the integrated HIV genome from cells to immunize the patient against viral re-infection (Lopez 2021). Although these strategies are often combined to treat HAND, some secondary side effects of cART can actually cause neurological disorders like HAND, anxiety, insomnia, and depression. These side effects can prevent patients from continuing cART, resulting in viral rebound and chronic infection of HIV (Lopez 2021).

Although cART strategies are successful at inhibiting HIV replication so that it is at undetectable levels, latent HIV persists in the body in reservoirs in the central nervous system, causing HAND. However, the mechanisms involved in activation of the latent virus and in the development of HAND are unclear. Studies have shown that successful stem cell transplantation with the delta CCR5 receptor removed, resulted in apparent clearance of HIV infection but it was still unclear whether the CCR5 deletion cleared viral reservoirs (Lopez 2021). Termination of cART treatments results in a rapid viral rebound that increases the viral load in the body to approximately the level of virus before cART treatment. Previous studies suggest the main reservoir to be CD4 T cells, as well as additional potential reservoirs including dendritic cells, bone marrow, and cell types in the brain such as astrocytes and microglial cells. Targeting these reservoirs of HIV in the brain and in cells of the central nervous system in vivo is challenging due to the blood-brain barrier (BBB), which can prevent drugs from reaching the reservoirs. The BBB blocks the exchange between the virus in the brain and the rest of the body, like the blood, which accounts for the resting levels of HIV detected in the body despite cART treatment (Wallet 2019).

Astrocytes, microglia, and macrophages are long lived unlike infected monocytes, which suggests these cell types are possible reservoirs of HIV. Microglia contain both CXC4 and CCR5 coreceptors which HIV-infected immune cells can bind to (Rojas-Celis 2019). It is also thought that microglia engulf HIV-infected CD4 T cells crossing the BBB into the brain, thereby creating a HIV reservoir in microglia (Wallet 2019). Upon infection, microglia can become activated and secrete cytokines causing neuroinflammation and increased reactive oxygen species (ROS) that could contribute to the pathology seen in HAND. Another cell type in the CNS thought to be infected by HIV are astrocytes. Lutgen et al. (2020) found that under cART, hippocampal astrocytes harbor HIV. However, the pathogenesis of infection of astrocytes is unclear. On the contrary, Ko et al. (2019), found HIV-1 to be detected in macrophages and microglia cells but not in astrocytes, therefore HIV-1 may not infect astrocytes but selectively infect microglia.

The mechanisms of HIV infection can be studied using the replication competent AD8 strain; and dEnv, a virus pseudotyped with an envelope from Vesicular Stomatitis Virus (VSV) that can act as a lentivirus and infect most cell types, but cannot replicate and spread infection like AD8 (Hastie 2013). I hypothesize that AD8 will selectively infect microglial cells, leading to reactive changes in astrocytes and neurons. I expect microglia infected with AD8 or dEnv will display altered proliferation and migration as well as increased activation and cytokine production that will elicit changes in the morphology of neurons, activate astrocytes, and alter synaptic connectivity.

Understanding how HIV works in microglia, astrocytes, and neurons in the CNS is challenging because of the limitations associated with manipulating these cells in vivo. In

addition, models such as mice do not accurately recapitulate the effects of HIV infection on the human brain, as the mouse brain is much simpler. By deriving microglia, astrocytes, and neurons from hPSCs, we are able to model HIV infection using a system that can be easily manipulated in ways that would be difficult to achieve in an in vivo system like the mouse. Doing these experiments on human cells can aid in the identification of mechanisms of viral infection in humans and creation of therapies for human patients. Furthermore, by optimizing differentiation of hPSC into astrocytes and neurons we can assess the cell-type specific effects of HIV in a controlled population of cells with fewer confounding variables.

In this study, it was first determined how HIV infection affects microglia function using established protocols previously optimized in the Novitch lab to produce hPSC-derived microglia. Microglia are known to respond to injury by proliferating, migrating to the site of injury, and producing various cytokines. Therefore, we measured proliferation and migration after HIV infection. These results showed a change in proliferation and migration of microglia after HIV infection that correlated with time and the presence of ADP. This suggests that HIV infection might inhibit microglial migration initially by decreasing the ADP signal in the environment, but as time progresses, the microglia are able to overcome inhibition and migrate to the site of infection in the presence of ADP.

As microglia can have effects on other cell types in the CNS, the next goal was to create a tri-culture system with microglia, neurons, and astrocytes. The production of neurons, and astrocytes from hPSCs was optimized by measuring expression of cell-type markers via immunohistochemistry (IHC) and gene expression levels with quantitative polymerase chain reaction analysis (qPCR) using a published protocol for tri-cultures with some modifications (Guttikonda et al. 2021). This resulted in successful differentiation of NPCs to neurons and astrocytes due to the cells displaying markers for neurons and astrocytes. I tested adding in microglia before the other cell types in order to accurately simulate the order the cells would appear during development.

Future studies will make use of the fact that dEnv cannot make virions, i.e. cannot spread infection to other cells. Using a tri-culture system with a single infected cell-type could be used to see which infected cells result in changes in neurons. With dEnv, I can target specific cell populations by infecting monocultures of microglia, astrocytes, and neurons, wait for the infectious particles to be taken up, and then mix the infected cells with the non-infected cells. Adding dEnv on to infected microglia, and then adding astrocytes and neurons to form the tri-culture here can be used to show a causal relationship between infected microglia and activation of astrocytes and changes in neurons. Along the same lines, dEnv could be used to infect only astrocytes with non-infected microglia and neurons to determine whether infected astrocytes can activate microglia and alter neurons. I hypothesize that these experiments will show that direct viral infection with dEnv in microglia can lead to indirect effects in astrocytes and neurons. Using AD8 with the tri-culture system, I will determine whether HIV selectively infects microglia and if it is possible for human astrocytes to be infected.

I predict that the hypothesized changes to neurons and synaptic activity by HIV will lead to the pathology associated with HAND. Using this model will provide a better understanding of the mechanisms underlying HAND. A better understanding will allow researchers to narrow down the therapeutic targets that could reverse or prevent HAND in patients and improve their quality of life.

Methods:

1. Human pluripotent stem cell (hPSC) maintenance:

Human pluripotent stem cells (line xeno-free induced pluripotent stem cells "XfiPSC") were obtained from the UCLA Broad Stem Cell Research Center and used with approval from the UCLA Embryonic Stem Cell Research Oversight (ESCRO) Committee. hPSCs were maintained in mTeSR (Stem Cell Technologies #85850) on hESC-qualified matrigel (Corning #354277) coated plates. hPSCs were passaged every 4-5 days or until they reached about 80-90% confluency and split at a dilution of 1:8-1:15 using ReLeSR (Stem Cell Technologies Catalog #05872) incubated for 1-2 minutes following the manufacturer's instructions. Briefly, hPSCs were washed with 2 mL/well PBS without calcium and magnesium. 200 uL/well of ReLeSR was then added dropwise. The plate was rocked back and forth and then the ReLeSR was aspirated. The hPSCs were then incubated for 1-2 minutes and checked at the microscope for edges to lighten and colonies to show small holes. The hPSCs were then lifted with 2 mL/well mTeSR, diluted to fresh matrigel plates, and media was changed daily with 2 mL/well mTeSR.

2. Differentiation of hPSCs to microglia:

When hPSCs reached 80-90% confluence, the cells were lifted with ReLeSR for 1-2 mins with minimal pipetting to achieve large colonies. To count the colonies, 5µL of colonies were placed in three wells of a 96-well flat bottom plate containing 45µL DMEM/F12 (Hyclone #SH30023.02). If there were greater than 1 colony per uL, the colonies were diluted further and counted again. It is ideal to have about one colony per microliter or less. 10-40 colonies were plated in 12-well plates coated with hESC-qualified matrigel (Corning #354277). The next day, the number of colonies per well were manually counted and only those with 10-25 large colonies were kept. The hPSCs were differentiated to hematopoietic stem cells according to the STEMdiff™ Hematopoietic Kit (Stem Cell Technologies #05310) with a few modifications.

At day 0, mTeSR was aspirated and the hPSCs were fed 1 mL/well Media A. On day 2, a half media change was performed where 500 uL/well was removed, and a fresh 500 uL/well of Media A was added. On day 3, all media was aspirated, and replaced with 800 uL/well Media B. On days 3, 5, 7, and 10, 400 uL/well Media B was added (no media was removed). On day 12, the floating cells were gently collected with wide bore p1000 tips or glass pipettes with minimal pipetting to avoid dislodging the HPC producing colonies. The floating cells were centrifuged at 300 g for 5 minutes at room temperature. 1 mL/well of conditioned media B was returned to the plates, and then a fresh 400 uL/well of Media B was added. The cells were counted, and 0.8-1.2x10^6 cells per vial were frozen in 1mL per vial BamBanker (Wako #NC9582225) and placed at -80 degrees overnight. The following day the vials were transferred to liquid nitrogen for long-term storage. The same procedure was repeated on days 14 and d16 for a total of three collections. We typically produced 30-40 million hematopoietic stem cells (HPCs) per STEMdiff™ Hematopoietic Kit (26 wells of a 12 well plate).

To produce microglia from frozen stocks of HPCs, a modified version of the 28 day protocol described in McQuade et al. (2018) was used. Microglia base media consisted of DMEM/F12 (Hyclone #SH30023.02) supplemented with 1x Insulin-Transferrin-Selenite (ITS-G, Invitrogen #4140004), 1x B27 with Vitamin A (ThermoFisher #17504044), 0.5x N2 (Invitrogen #18091050), 1x Glutamax (ThermoFisher #35050-061), 1x MEM Non-Essential Amino Acids Solution (NEAA, ThermoFisher #11140050), 5 ug/mL Insulin (Sigma #I2643-50MG), and 400 uM Monothioglycerol (Sigma #M1753-100ML). Microglia based media supplemented with three

cytokines “MG+3c” consisted of Microglia base media 100 ug/mL IL-34 (Peprotech #200-34), 50 ug/mL TGFB1 (Peprotech #100-21), and 100 ug/mL M-CSF (Peprotech #300-25). Microglia base media supplemented with five cytokines “MG+5c” consisted of MG+3c with 100 ug/mL CD200 (BioLegend #770004) and 100 ug/mL CX3CL1 (Peprotech #300-31). Cytokines were added fresh each time, and multiple freeze/thaws were avoided as it reduces their activity. Cytokine aliquots were maintained at 4 degrees for up to one week.

HPCs were thawed according to BamBanker’s thawing instructions. Cells were thawed in warm tap water without shaking and then its contents were transferred to a 15 mL conical tube. Next, 10 mL of microglia base media was added dropwise. The conical tube was slowly inverted once, and then centrifuged at 300 g for 5 minutes at room temperature. The media was aspirated and cells were resuspended in 1 mL MG+3c and counted. 25,000 cells/well were added to 6-well plates coated with 1 mg/mL Corning® Matrigel® Growth Factor Reduced (GFR) Basement Membrane Matrix (Corning #354230). On days 2, 4, 6, 8, and 10, 1 mL/well MG+3c was added (no media removed). On day 12, all the media was gently picked up and 1 mL/well conditioned media was then replaced back to the plates. The rest of the media in the conical tube was centrifuged at 300 g for 5 minutes at room temperature. After centrifuging, all media was aspirated, and the cells were resuspended in 1 mL/well fresh MG+3c and 1 mL/well was added on top the conditioned media such that each well contained 1 mL conditioned media and 1mL fresh MG+3c. On days 14, 16, 18, 20, 22, and 24, 1 mL/well MG+3c was added (no media removed). On day 26, the media was gently picked up and centrifuged at 300 g for 5 minutes at room temperature. After centrifuging, all media was aspirated and the cells were resuspended in 2mL/well MG +5c (no conditioned media kept). On day 28, 1mL per well MG +5c was added (no media removed). On day 29 the cells were ready for use and could be maintained in MG +5c for up to two additional weeks.

3. iPS-microglia infection and functional assays:

To infected hPSC-microglia, the cells were lifted from plates with accutase and incubated 4-5 minutes at 37 degrees. When the cells were in suspension, a “spinfection” was performed which consisted of centrifuging the cells for an hour in the presence of HIV. Then, the cells were plated in 6-well plates. After 2, 4, or 6 days, the cells were then lifted again and an ADP migration assay was performed using transwell inserts using the protocol described in McQuade et al. (2018).

For proliferation assays, we replated the cells at 50K/well microglia to chamber plates in 500uL/well MG+5c. Two days later, we fed the cells by adding 250uL/well on top (no media removed). Two days after that we removed all media, and bath applied the virus in 500uL/well fresh culture media +5c and incubated for 24 hours. After 24 hours, the virus was removed by performing a full media change to a fresh 500uL/well MG+5c and/or experiments with the Click-it EdU Cell Proliferation Kit. Then, imaging (Invitrogen 10337) was performed according to the manufacturer's instructions with a 2 hour EdU incubation.

3. Differentiation of hPSCs to neural progenitor cells (NPCs):

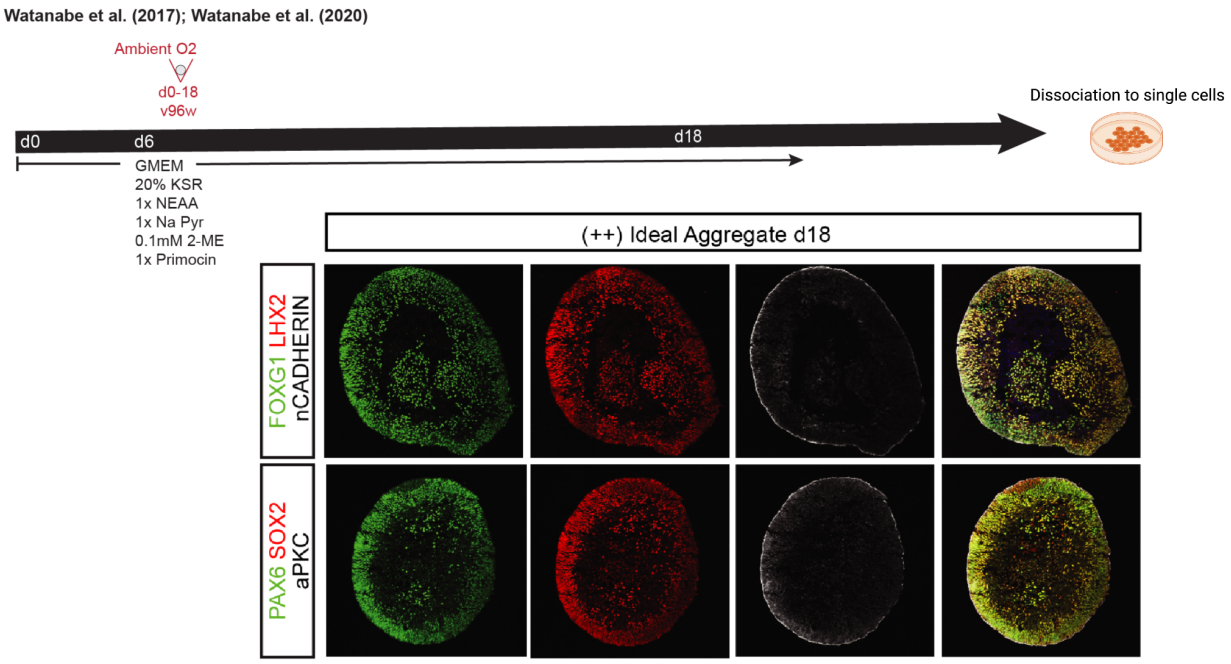

Figure 1. NPCs derivation from organoids after dissociation to single cells on day 18.

We optimized deriving neurons and astrocytes from neural progenitor cells (NPCs) and used our previously made microglia (MG) batches in order to add these grown neurons, astrocytes, and microglia for the tri-culture experiments. We derived NPCs from 18 day old iPSC-brain organoids using the Novitch lab's protocol for brain organoids (Watanabe et al. 2017). At this stage, brain organoids are made up of a ball of FOXG1+/LHX2+ neural progenitor cells shown by immunostaining for FOXG1 and LHX2 positive neural progenitor cells **(Fig. 1)**. First, we dissociated the organoids to single cells by collecting with wide bore tips to a 15 mL conical tube. Media was removed with a p1000, and then washed with 2 mL PBS without calcium/magnesium. Next, 1900µL accutase with 100µL DNase1 was added to the organoids and incubated for 5 minutes at 37 degrees. The organoids were then pipetted 5-10 times with a p1000 to break up to single cells. Next, 8 mL of media was added and the cells were mixed up and down once. Any clumps were then removed by filtering the cells through a 100 um mesh cell strainer (Fisher 22-363-549). Then, the cell solution was centrifuged at 180 g for 5 minutes room temperature. After centrifuging, all media was aspirated and the cells were resuspended in NPC media supplemented with 20 ng/mL FGF and 20 ng/mL EGF and counted. 500 mL of NPC media consisted of 240mL of 50% DMEM/F12 (Hyclone Cytiva), 240mL of 50% Neurobasal (Gibco), 2.5mL of 0.5 × N2 (100x Life Technologies 17502-048), 5mL of 0.5 × B27 without VA (50x Gibco, 12587-010), 5mL of 1% Glutamax (100x Gibco 35050-061), 5mL of 1% NEAA (100X Gibco), 500µL of 5 µg mL−1 insulin (Sigma), 1mL of Primocin (stock 500x, InvivoGen ant-pm-2 or ant-pm-1), and 100µL of 1 µg mL−1 Heparin (10mg/ml stock Sigma H3419-100KU) (Shan et al. 2020). 100,000 cells/well were added to 6-well plates coated with Matrigel (Fisher

Scientific, #CB-40230), and media was changed every other day with 2 mL/well NPC expansion media. NPC expansion media was supplemented with 20 ng/mL basic fibroblast growth factor (bFGF), and 20 ng/mL epidermal growth factor (EGF) (Peprotech AF-100-15). After seven days, the cells were passaged 1:2-1:3 to new matrigel coated dishes. After the 7 days, the cells were washed with PBS without calcium/magnesium and then lifted using 1 mL/well accutase for 5 minutes at 37 degrees. Next, the plate was tapped to loosen the cells, and then lifted to a 50 mL conical tube with NPC media. The cells were counted, and then frozen down into vials with 1 million cells/vial in 1 mL/vial bambanker (Wako NC9582225).

4. Differentiation of NPCs to neurons and astrocytes:

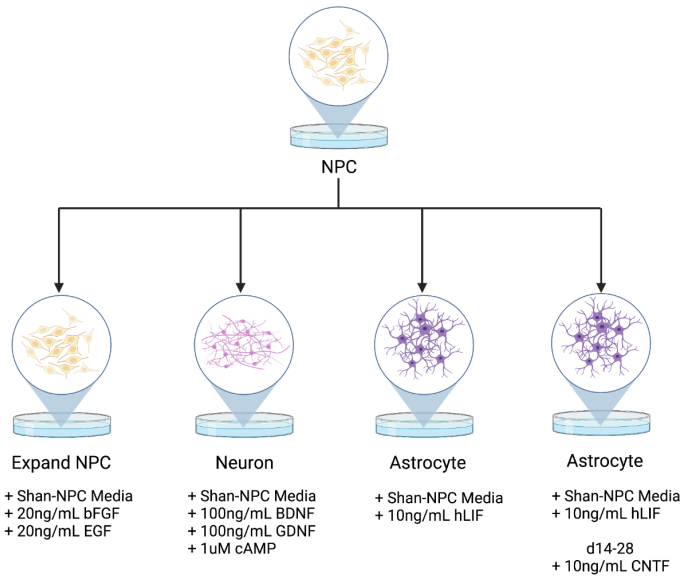

Figure 2. Schematic of neural progenitor cell (NPC) differentiation to various cell types. From left to right to figure shows, the media to maintain NPCs (Expand NPC), differentiation to neurons (Neuron), or two methods tested to differentiate NPCs to astrocytes (LIF-Astrocyte and CNTF-Astrocyte).

For NPC differentiation to neurons or astrocytes, on day (-4), we thawed NPCs to 6-well plates coated with 1:20 Matrigel/DMEM-F12 with 100K cells/well. On d(-2), a full media change was performed and 2 mL/well of fresh NPC expansion media (NPC supplemented with 20 ng/mL FGF and 20 ng/mL EGF) was added to let the cells recover and expand (**Fig. 2 "Expand NPC"**).

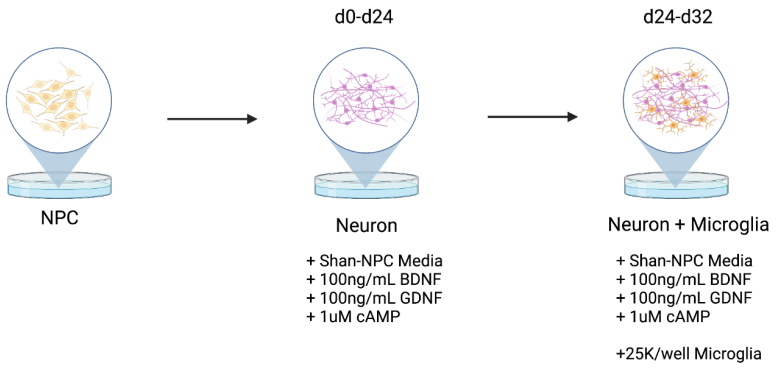

Figure 3. Schematic of microglia addition to neuron cultures.

For neuron differentiation, on day 0-28, the cells were fed "Neuron media" every other day which consisted of NPC media supplemented with 100 ng/mL of brain-derived neurotrophic factor (BDNF, Peprotech 450-02), 100 ng/mL of glial-derived neurotrophic factor (GDNF, Peprotech 450-10), and 1uM cyclic AMP (cAMP, Sigma #D0260-5MG) (**Fig. 2 "Neuron"**). When the cells reached 95% confluence on day 8-10, the cells were passaged 1:2-1:3 using accutase and DNase1 as described in the methods section 3 (NPC production). To enrich the culture with neurons, on day 20, 20 ng/mL Mitomycin C (Sigma #M4287-2MG) was added for 2 hours. This caused the majority of remaining neural progenitors to die off over the next 4-6 days while preserving the differentiated neurons. On day 24 of the 28 day differentiation protocol, 25K/well of microglia were added to wells of the Neuron dish by adding cells in 250µL Microglia base media supplemented with 100 ng/mL IL-34, 50 ng/mL TGFB1, 100 ng/mL M-CSF, 100 ng/mL CD200, and 100 ng/mL CX3CL1 "MG+5c" or MG+5c media alone on top of the neuron media (**Fig. 3**). Then, on day 26 a full media change was performed with fresh neuron media (no MG media or cytokines) and fed every other day up until day 32 (**Fig. 3**).

For astrocyte differentiation, we tested two conditions: For "LIF-Astrocyte", the cells were fed NPC media supplemented with 10 ng/mL human leukemia inhibitory factor (hLIF) (Peprotech #300-05) every other day for 28 days, or for "CNTF-Astrocyte", the cells were fed NPC media supplemented with 10 ng/mL hLIF every other day for 14 days followed by 10 ng/mL hLIF with 10 ng/mL ciliary neurotrophic factor (CNTF) (Peprotech #450-13) every other day from day 14-28 (**Fig. 2 "Astrocyte"**).

Table 1. Antibodies used for immunostaining.

Antibody	**Host**	**Conjugated**	**Company**	**Catalog #**	**IHC Dilution**
Neural Progenitors					
SOX2	Goat	--	R&D	AF2018	1:100

PAX6	Rabbit	–	MBL	PD022	1:1000
NESTIN	Mouse	–	Neuromics	M015012	1:1000
FOXG1	Rabbit	–	Abcam	ab18259	1:1000
LHX2 (Clone C-20)	Goat	–	Santa Cruz Biotech.	sc19344	1:1000
Microglia					
CX3CR1	Rat	PE	Biolegend	341604	1:200
IBA1	Rabbit	--	Wako	019-19741	1:500
Astrocyte					
HepaCAM	Mouse	--	R&D	MAB4108	1:500
HepaCAM	Sheep	–	R&D	AF4108	1:200
S100b	Rabbit	--	Fitzgerald	F DI-S100Babr	1:1000
GFAP	Rabbit	--	Abcam	Ab7620-50	1:1000
Neuron					
TUJ1	Mouse	--	Biolegend	801202	1:10000
MAP2	Chicken	--	NovusBio	NB300-213	1:5000
HIV					
p24	Mouse	PE	Beckman Coulter	6604665 (KC57-FITC)	1:500

Table 2. qRT-PCR Primers used.

Gene	**Primer Sequence**
Beta-actin	Forward 5'-GATCAAGATCATTGCTCCTCCT-3' Reverse 3'-GGGTGTAACGCAACTAAGTCA-5'
PAX6	Forward 5'-TGTCCAACGGATGTGTGAGTA-3' Reverse 3'-CAGTCTCGTAATACCTGCCCA-5'
SOX2	Forward 5'-GCCGAGTGGAAACTTTTGTCG-3' Reverse 5'-GGCAGCGTGTACTTATCCT-3'

6. Immunostaining and quantitative real-time polymerase chain reaction (qRT-PCR) analysis:

Immunostaining and *qRT-PCR* were performed as described in Watanabe et al. (2017). Antibodies used in this study are listed in Table 1. For RNA extraction, the Qiagen miRNeasy Tissue/Cells Advanced Microkit was used (Qiagen #217684). For RNA to cDNA conversion, the Superscript IV kit was used (Invitrogen #18091050). For qRT-PCR, SYBR green dye was used with the primers shown in Table 2. Fold change was calculated using the delta-delta Ct method.

Results:

1. Effects of HIV-infection on microglial function

Microglia are known to respond to injury by multiplying, migrating to the site of injury, and producing various cytokines. Therefore, we expected the amount of proliferating cells following infection with dEnv to increase. We found a higher percentage of p24+ cells compared to virtually no p24+ cells in the uninfected control, indicating successful infection of on average 20-30% of the microglia. (**Fig. 4A-B**). There was a trend that the percentage of Ki67+ and EdU+ cells after 24 hour incubation with dEnv is greater than in the uninfected condition (**Fig. 4B**).

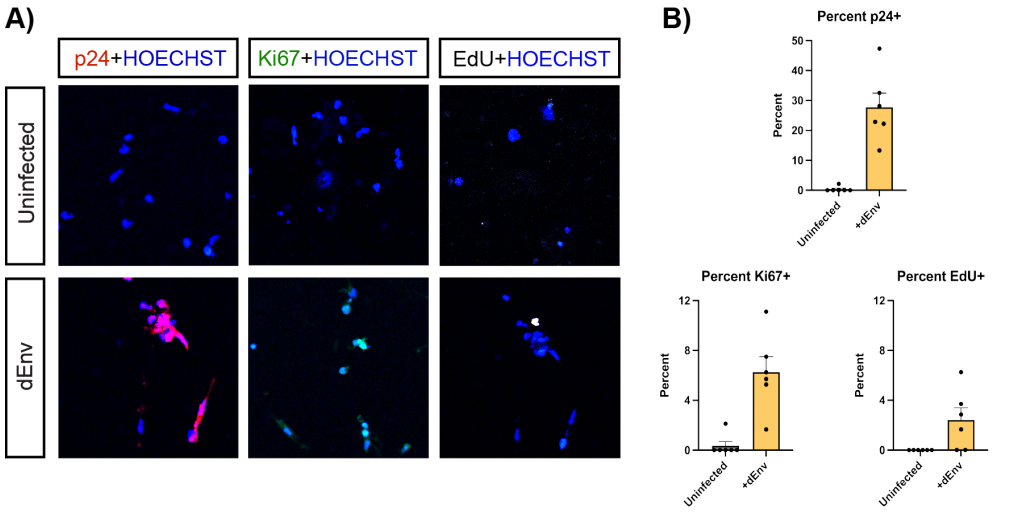

Figure 4: **Proliferation analysis reveals that cells infected with dEnv proliferate less than uninfected cells. (A)** P24 in redCy3 marks HIV, Ki67 in greenA488 marks any cell that is not in the G0 phase of the cell cycle, EdU in whiteA647 marks any cells that synthesized DNA during EdU incubationis in the S phase of the cell cycle, and HOECHST in blue marks all nuclei. **(B)** Percent of cells positive for the different markers divided by total cells. Mean with SEM is shown. n=6 per condition.

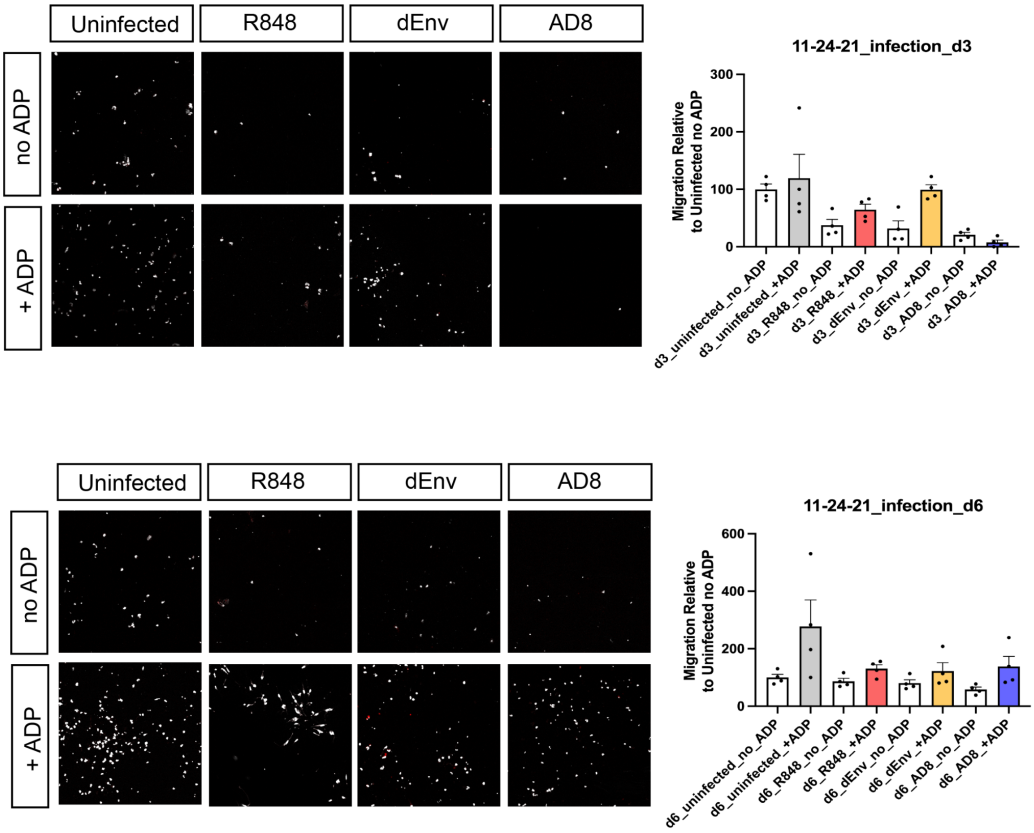

Figure 5. **ADP Migration Assay of 11-24-21 infection on day 3 and day 6 shows an increase in migration rate of microglia infected by AD8 in the presence of ADP from day 3 to day 6.**

An ADP migration assay was performed according to the protocol described in McQuade et al. (2018). Fixing the cells on day 3 shows that in the absence of ADP, the migration rate of cells is the highest when they are uninfected and decreases when the cells are infected with the inflammatory stimulus R848, dEnv, and AD8. This is in contrast to the cells fixed on day 6 in the absence of ADP, as the migration rate does not change across uninfected and infected conditions. In the presence of ADP on day 3, the uninfected cells and cells infected with dEnv had comparable migration rates to the uninfected cells in the absence of ADP. Day 3 cells infected with R848 had a decreased rate of migration in the presence of ADP and cells infected with AD8 had the lowest migration rate. In the presence of ADP on day 6, the migration rate of uninfected cells doubled compared to the migration rate of uninfected cells in the absence of ADP. The migration rate of day 3 and day 6 R848 infected cells in the presence of ADP did not change, but the migration rate of day 6 dEnv infected cells in the presence of ADP decreased compared to day 3 cells. There was an increase in the migration rate of day 6 AD8 infected cells in the presence of ADP compared to the day 6 AD8 infected cells in the absence of ADP. The migration rates for the R848, dEnv, and ADP infected cells were similar to each other on day 6.

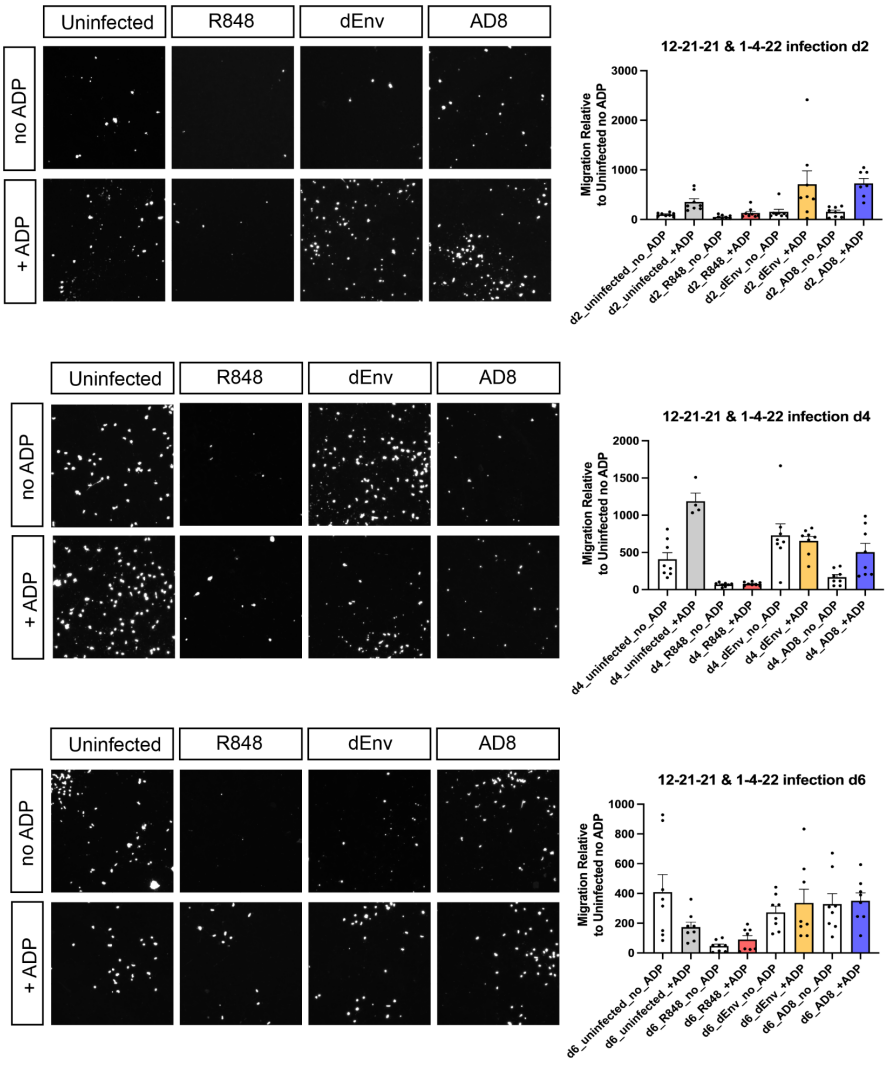

Figure 6. **ADP Migration Assay of 12-21-21 infection and 01-04-22 day 2, day 4, and day 6.**

Day 4 and day 6 cells had higher migration rates for all conditions than day 2 cells. Fixing cells on day 2 shows that uninfected, R848 infected, and dEnv infected cells have very low migration rates in the presence or absence of ADP. Day 4 and day 6 cells have low migration rates for the R848 infected cells in the presence or absence of ADP, but the day 4 cells have a significantly higher rate of migration for the uninfected cells in the presence of ADP compared to day 2 and day 6 cells. Day 6 cells have a high rate of migration for the uninfected cells in the absence of ADP. The migration rate of dEnv and AD8 in the presence of ADP decreases across all 3 days. There is no change in the migration rate of dEnv in the presence

and absence of ADP on day 4 and day 6, and no change in migration rate of AD8 in the presence and absence of ADP on day 6.

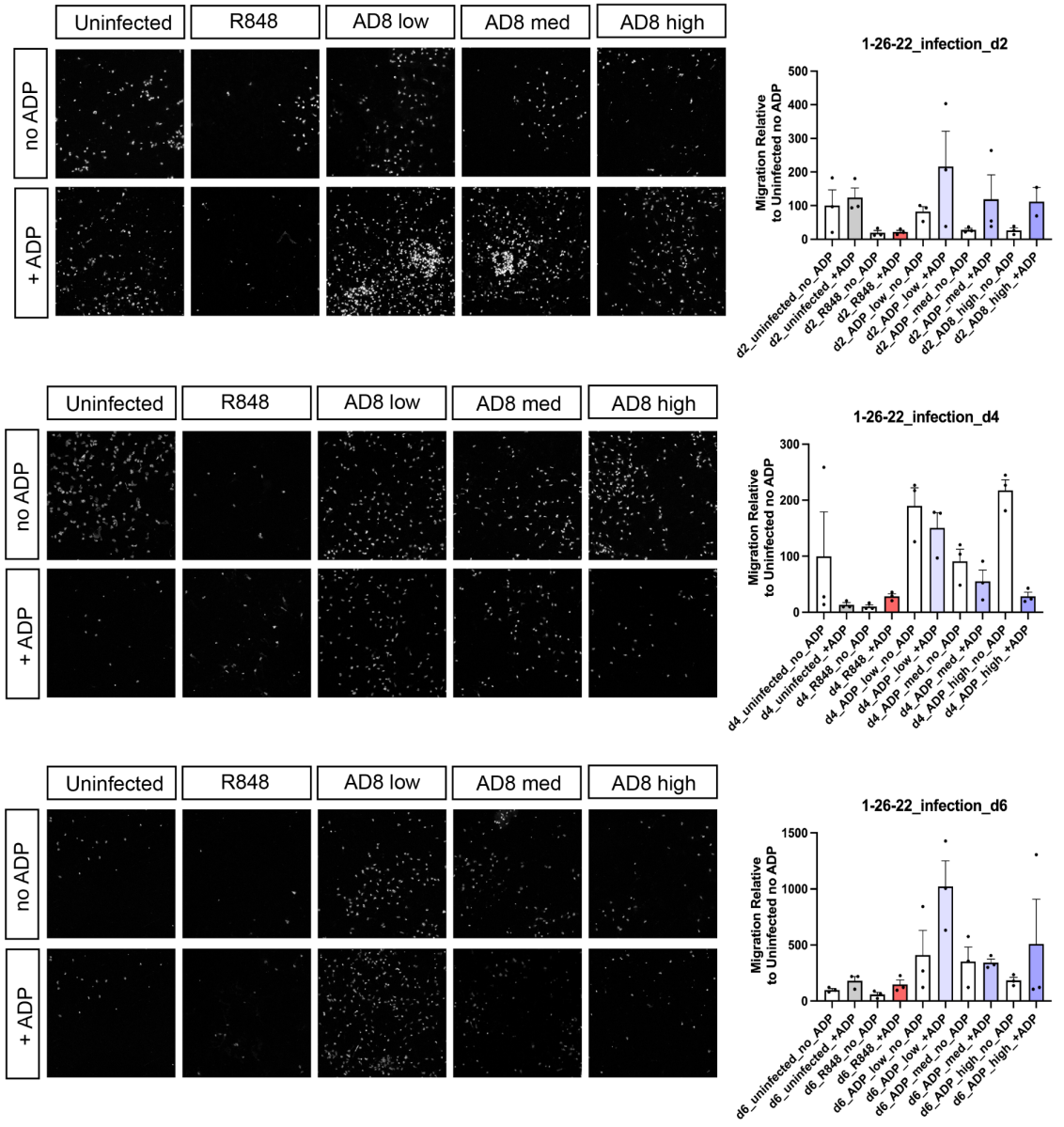

Figure 7. ADP Migration Assay of 01-26-21 infection day 2, day 4, and day 6.

The cells were infected with R848 and low, medium, and high concentrations of AD8. Cells fixed on day 2 had the fastest migration rate when they were infected with a low concentration of AD8 in the presence of ADP. Increasing the concentration of AD8 infection decreased the rate of migration in the presence and absence of ADP. Cells infected with R848

in the presence of ADP had similar migration rates across all 3 days and had a very low migration rate in the absence of ADP across all 3 days. Uninfected cells in the presence and absence of ADP had no change in migration rates on day 2, but uninfected cells in the absence of ADP had a greater migration rate on day 4 compared to cells in the presence of ADP and uninfected cells on day 2 and day 6. Day 4 cells in the absence of ADP had similar high migration rates when infected with a low concentration of AD8 and a high concentration of AD8. Day 6 cells infected with a low concentration of AD8 in the presence of ADP have the highest rate of migration compared to other day 6 cells. Migration rates for cells infected with high concentrations of AD8 in the presence of ADP decrease from day 2 to day 4 but increase from day 4 to day 6.

2. Derivation of NPCs from organoids for 2D culture

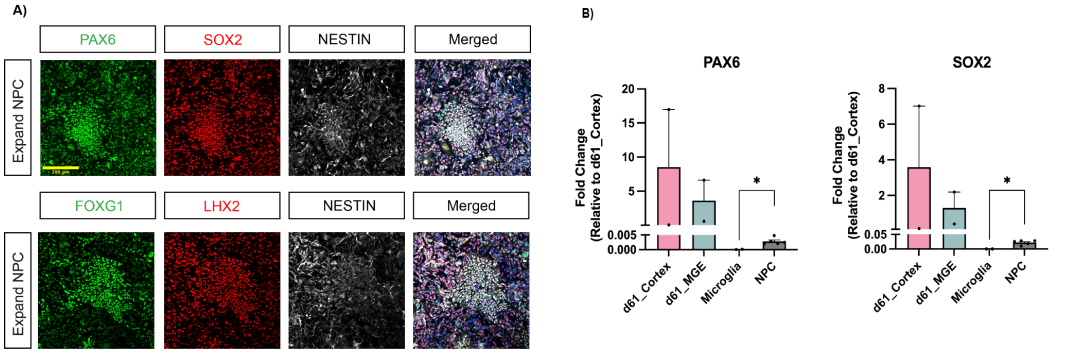

Figure 8. NPCs maintained in NPC expansion media maintain cortical NPC markers and dorsal forebrain identity. (A) Immunostaining of neural stem cell markers (PAX6, SOX2, and NESTIN) and dorsal forebrain markers (FOXG1 and LHX2). Scale bar = 200 um. (**B)** qRT-PCR for neural stem cell markers (PAX6 and SOX2) in neural progenitor cells "NPCs" were compared to positive controls 61 day old iPSC-derived cortical organoids "d61_Cortex" (high PAX6 and SOX2), 61 day old medial ganglionic eminence organoids "d61_MGE" (PAX6 and SOX2 expressed, but lower than cortical organoids), and negative control iPSC-derived microglia (PAX6 and SOX2 not expressed). Values shown are mean + SEM. Fold change was normalized to the d61_Cortex condition. n are as follows: d61_Cortex n=2; d61_MGE n=2; Microglia n=2; NPC n=5. Welch's ANOVA with Dunnett's multiple comparisons was performed. Asterisks denote * = $p < 0.05$, ** = $p < 0.01$, *** = $p < 0.001$, **** = $p < 0.0001$.

NPCs were derived from organoids for 2D culture and a future tri-culture model and maintained in NPC expansion media. Immunostaining for neural progenitor markers showed cells positive for the following neural progenitor markers: PAX6, SOX2, FOXG1, LHX2, and NESTIN (**Fig. 8A**). QRT-PCR for neural stem markers shows significant upregulation of PAX6 and SOX2 for the NPCs compared to microglia, which do not express PAX6 and SOX2. Gene expression by the NPCs was less than the d61 Cortex organoids, which have high expression of PAX6 and SOX2, and d61 MGE organoids, which have moderate expression of PAX6 and SOX2 (**Fig. 8B**).

3. Optimization of protocols to produce cortical neurons and astrocytes from NPCs

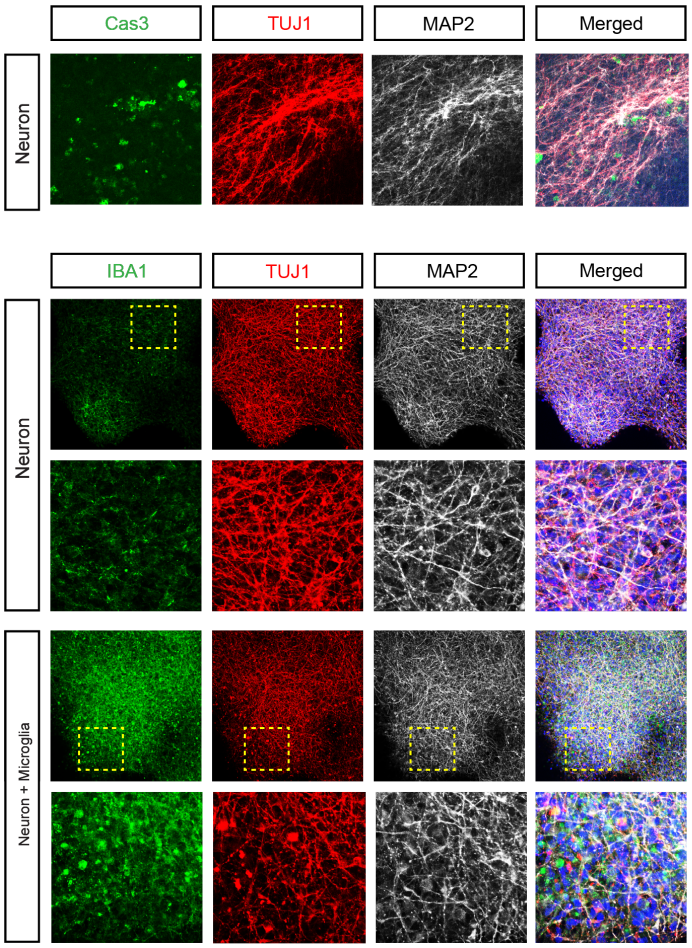

Figure 9. Microglia can integrate and survive in neuron cultures. NPCs in the presence or absence of microglia immunostained for neuronal markers (TUJ1 and MAP2), microglial markers (IBA1), and cell death (Cas3)..

Next, protocols to produce neurons and astrocytes were optimized. In the absence of microglia, there were an abundance of neurons positive for TUJ1 and MAP2 with few dead cells positive for cleaved caspase 3 (Cas3), and no noticeable cells positive for IBA1 present (**Fig. 9**). In the presence of microglia, cells positive for IBA1 had integrated and survived in the culture for at least seven days without cytokines present. Last, we aimed to improve protocols to produce astrocytes. As it's known STAT3 signaling is important for astrogliogenesis, two STAT3 activators were tested; LIF and CNTF (Chandrasekaran et al. 2016). It was tested whether LIF alone for 28 days or LIF for 28 days with CNTF for d14-28 would produce more astrocytes. We

found there are more astrocytes in the CNTF-astrocyte condition that are positive for GFAP and HepaCAM compared to the LIF-astrocyte condition (**Fig. 10**).

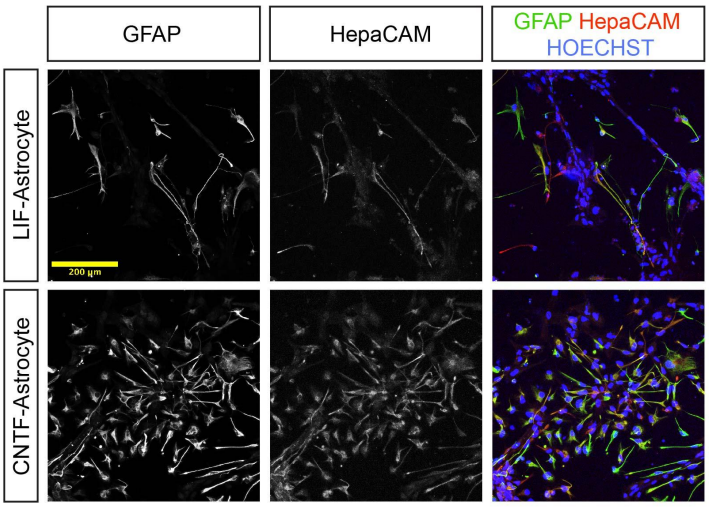

Figure 10. Addition of CNTF improves astrocyte differentiation. NPCs differentiated to astrocytes immunostained for astrocyte/NPC marker (GFAP) and mature astrocyte specific marker (HepaCAM).

Discussion:

1. Effects of HIV-infection on microglial function:

When microglia are infected with dEnv, there's a lower percentage of cells that are not in the G0 phase of the cell cycle which indicates that there are more cells in the G0, or the quiescent phase (**Fig. 4A**). This phase of the cell cycle involves the cell in a resting state until it receives growth factors that signal continuation through the cell cycle. Furthermore, there are fewer cells in the S phase when the cells are infected with dEnv, which means less DNA is being replicated (**Fig. 4A**). Without complete DNA replication, checkpoints after the S phase prevent progression of the cell through the cell cycle. Therefore, microglia are not proliferating in the presence of an HIV-simulated infection by dEnv because of the regulation of the G0 and S phases in the cell cycle. The proliferation of other cell types of the central nervous system, including neurons and astrocytes, can be affected in similar ways in response to HIV infection. The growth arrest experienced by microglia cells can be experienced by neurons and astrocytes in the presence of HIV which can explain how HIV evades the host immune response in the brain and causes HAND. The decrease in microglia and astrocyte growth results in the body being unable to fight off HIV infection in the brain, resulting in the death of neurons. Neuron death causes HAND because of the decrease in synapses that relay the neurotransmitters needed for memory, movement, and homeostasis.

When there is no ADP present, on day 3, uninfected microglia cells have the fastest migration rate and the migration rate decreases when the cells are infected (**Fig. 5A**). This suggests that infection by HIV decreases microglia migration to the site of infection initially. This

is in contrast to the cells fixed on day 6 in the absence of ADP, as the migration rate does not change across uninfected and infected conditions (**Fig. 5A**). Therefore, microglia migration rate is dependent on time and stabilizes for uninfected and infected microglia as time increases when ADP is not present. However, when ADP is present, the rate of microglia migration increases for uninfected and infected microglia, except for the AD8 infected cells on day 3. The increase in migration rate for the AD8 infected cells from day 3 and day 6 in the presence of ADP suggests that microglia respond to ADP in the environment at a later time point. Evaluating more time points reveals that microglia cells have a fast rate of migration when they are uninfected and in the presence of ADP on day 4 (**Fig. 5B**). This is possibly due to ADP acting as a signal in the environment for microglia migration. The migration rate of dEnv and AD8 in the presence of ADP decreases across all 3 days. This might be because HIV infection inhibits microglial migration initially by decreasing the ADP signal in the environment, resulting in a decrease in microglia migration to the site of infection.

Varying the concentrations of AD8 shows a decrease in microglia migration rate in infected cells as time increases in the absence of ADP (**Fig. 5C**). This might be because microglia may be able to migrate in an ADP-independent manner initially, but need ADP to migrate at later time points. Low ADP concentration and high ADP concentration decrease the migration rate of microglia from day 2 to day 4, but increase migration rates from day 4 to day 6 (Fig. 4C). This suggests that any ADP concentration can contribute to fluctuations in microglia migration rate.

2. Maintenance of NPC identity in 2D culture:

After we freezed, thawed, and imaged the undifferentiatedNPCs using immunostaining, we found successful maintenance and expansion of NPCs. Following a 28 day expansion in NPC media supplemented with 20ng/mL of bFGF, and 20ng/mL of EGF, the NPCs maintained expression of neural progenitor markers PAX6, SOX2, and NESTIN (**Fig. 8A-B**). In addition, the NPCs maintained the regional identity of the cortical organoids they were derived from. In NPC expansion media, the cells displayed co-expression of dorsal forebrain markers FOXG1 and LHX2 similar to if they were kept in cortical organoids (**Fig. 8A**). Since NPCs from a cortical organoid maintained cortical identity, this suggests that NPCs from an MGE organoid could maintain an MGE identity. An MGE organoid can make interneurons which are responsible for GABAergic or inhibitory activity in the brain. Dysfunctional inhibitory neuron activity contributes to many neurodegenerative disorders including Parkison's disease which is caused by the inhibitory activity of dopaminergic neurons.

A follow-up study can be done by applying these conditions to an MGE organoid to create a possible 4-culture model with inhibitory neurons present. This could be used to assess crosstalk between the different cell types, network activity, and potential drug targets. In the 4-culture model, there would be conditions with and without inhibitory neurons to show how their activity is influenced by HIV or by other cells infected with HIV similar to methods done in cortex-MGE fusion organoids in Samarasinghe et al. (2021).

3. Neurons are sufficient to maintain microglia in 2D culture:

The optimal conditions tested to for differentiating NPCs to neurons were NPC media supplemented with 100ng/mL of brain-derived neurotrophic factor (BDNF), 100ng/mL of

glial-derived neurotrophic factor (GDNF), and 1uM cyclic AMP (cAMP) for a 28 day differentiation protocol. These conditions resulted in successful differentiation of NPC to neurons as the cells were positive for the pan neuronal markers TUJ1 and MAP2 (**Fig. 9)**. We assessed the survival of IBA1 positive microglia in the presence and absence of neurons and found that microglia cultured with cytokines for an initial two days during integration, survived one week without the five cytokines used to maintain them in culture alone survived in the presence of neurons, but died without these cytokines when cultured alone. This suggests the neurons are producing sufficient levels of these cytokines to maintain microglia in culture for at least one week (latest time-point measured). This finding is ideal for the tri-culture model in future experiments because adding cytokines can confound the measurement of cytokines produced by cells in response to HIV infection. Since neurons can sustain microglia in culture without the addition of cytokines, measuring the production of cytokines by microglia through an enzyme linked immunosorbent assay (ELISA) will clearly show the immune response to infection by microglial cells. In addition to a 2D tri-culture model, cytokine production in response to HIV infection can be measured in an organoid model in order to assess crosstalk and cell-cell contacts as a result of cytokine signaling.

4. Combined LIF and CNTF treatment promotes differentiation of mature HepaCAM+ astrocytes:

Astrocytes are the most abundant glial cells in the CNS. Astrocytes perform a variety of functions including monitoring the formation, maintenance, and engulfment of synapses, release of various cytokines, promote neuronal survival with release of neurotrophic factors, regulate neurotransmitter recycling at the synapse, cross-talk with neurons and microglia, and are involved in blood-brain barrier homeostasis (Engel 2016). Mature astrocytes produce cytokines upon activation, neurotrophic factors, and clear glutamate from the synaptic cleft using the glutamate transporter GLT1 (also known as SLC1A2 or EAAT2), decrease the level of proliferation, and change morphology to display elongated branches and smaller cell bodies compared to younger astrocytes (Sloan 2017). Many culture protocols, including stem cell differentiation to astrocytes, produce cells exhibiting fetal characteristics due to immature cells being differentiated from stem cells and sustained in culture. Immature astrocytes are not an accurate model because they are phenotypically different when infected in comparison to mature astrocytes (Chandrasekaran 2016)). Therefore, we tested two conditions for differentiation of NPC to astrocytes In order to determine the optimal conditions for differentiating NPC to mature astrocytes: “LIF-astrocyte” used NPC media with 10ng/mL hLIF for 28 days, and “CNTF-astrocyte” had the same amount of LIF for 28 days, but also had 10 ng/mL CNTF from day 14 through 28. Immunostaining of this experiment showed successful differentiation of NPC to astrocytes in both conditions, however, in the CNTF-astrocyte condition there were more cells positive for GFAP and HepaCAM (**Fig. 10**). Since GFAP can also stain NPCs, in order to more definitively assess the efficiency of astrocyte differentiation we stained for the astrocyte specific marker HepaCAM (Engel 2016).

LIF and CNTF were added to the media used in NPC differentiation to astrocytes because STAT3 signaling is known to promote astrocyte differentiation from radial glia and NPCs. The immunohistochemistry in Figure 10 showed increased expression of HepaCAM suggesting CNTF could be used to increase astrocyte maturation. Astrocyte maturity can be

assessed by the expression of specific markers, the level of proliferation, as well as changes in morphology over time. I will follow-up and further assess the maturation of the astrocytes in the LIF and CNTF-astrocyte conditions.

In the next quarter, I will follow up these results to characterize the maturity/activation of LIF-astrocytes and CNTF-astrocytes using immunostaining, qPCR, or ELISA to measure gene expression and cytokine/neurotrophic factor production, EdU to measure proliferation, and morphological changes with the ImageJ plugin, FracLac, which can measure complex cell morphologies (Karperien, FracLac 1999-2013). Once characterized, I will then measure if direct infection with HIV (dEnv) or indirect effects from HIV-infected microglia (dEnv or AD8) alter these measurement profiles.

References:

Borrajo López, Ana, Maria Aránzazu Penedo, Tania Rivera-Baltanas, Daniel Pérez-Rodríguez, David Alonso-Crespo, Carlos Fernández-Pereira, José Manuel Olivares, and Roberto Carlos Agís-Balboa. "Microglia: The Real Foe in HIV-1-Associated Neurocognitive Disorders?" *Biomedicines* 9, no. 8 (July 30, 2021): 925. https://doi.org/10.3390/biomedicines9080925.

Chandrasekaran, Abinaya, Hasan X. Avci, Marcel Leist, Julianna Kobolák, and Andras Dinnyés. "Astrocyte Differentiation of Human Pluripotent Stem Cells: New Tools for Neurological Disorder Research." *Frontiers in Cellular Neuroscience* 10 (September 26, 2016). https://doi.org/10.3389/fncel.2016.00215.

Engel, Martin, Dzung Do-Ha, Sonia Sanz Muñoz, and Lezanne Ooi. "Common Pitfalls of Stem Cell Differentiation: A Guide to Improving Protocols for Neurodegenerative Disease Models and Research." *Cellular and Molecular Life Sciences* 73, no. 19 (October 2016): 3693–3709. https://doi.org/10.1007/s00018-016-2265-3.

Guttikonda, Sudha R., Lisa Sikkema, Jason Tchieu, Nathalie Saurat, Ryan M. Walsh, Oliver Harschnitz, Gabriele Ciceri, et al. "Fully Defined Human Pluripotent Stem Cell-Derived Microglia and Tri-Culture System Model C3 Production in Alzheimer's Disease." *Nature Neuroscience* 24, no. 3 (March 2021): 343–54. https://doi.org/10.1038/s41593-020-00796-z.

Hastie, Eric, Marcela Cataldi, Ian Marriott, and Valery Z. Grdzelishvili. "Understanding and Altering Cell Tropism of Vesicular Stomatitis Virus." *Virus Research* 176, no. 1 (September 1, 2013): 16–32. https://doi.org/10.1016/j.virusres.2013.06.003.

Ko, Allen, Guobin Kang, Julian B. Hattler, Hadiza I. Galadima, Junfeng Zhang, Qingsheng Li, and Woong-Ki Kim. "Macrophages but Not Astrocytes Harbor HIV DNA in the Brains of HIV-1-Infected Aviremic Individuals on Suppressive Antiretroviral Therapy." *Journal of Neuroimmune Pharmacology* 14, no. 1 (March 2019): 110–19. https://doi.org/10.1007/s11481-018-9809-2.

Lutgen, Victoria, Srinivas D. Narasipura, Hannah J. Barbian, Maureen Richards, Jennillee Wallace, Roshanak Razmpour, Tetyana Buzhdygan, et al. “HIV Infects Astrocytes in Vivo and Egresses from the Brain to the Periphery.” Edited by Guido Silvestri. *PLOS Pathogens* 16, no. 6 (June 11, 2020): e1008381. https://doi.org/10.1371/journal.ppat.1008381.

McQuade, Amanda, Morgan Coburn, Christina H. Tu, Jonathan Hasselmann, Hayk Davtyan, and Mathew Blurton-Jones. “Development and Validation of a Simplified Method to Generate Human Microglia from Pluripotent Stem Cells.” *Molecular Neurodegeneration* 13, no. 1 (December 2018): 67. https://doi.org/10.1186/s13024-018-0297-x.

Rai, Mohammad A., Jason Hammonds, Mario Pujato, Christopher Mayhew, Krishna Roskin, and Paul Spearman. “Comparative Analysis of Human Microglial Models for Studies of HIV Replication and Pathogenesis.” *Retrovirology* 17, no. 1 (December 2020): 35. https://doi.org/10.1186/s12977-020-00544-y.

Rojas-Celis, Victoria, Fernando Valiente-Echeverría, Ricardo Soto-Rifo, and Daniela Toro-Ascuy. “New Challenges of HIV-1 Infection: How HIV-1 Attacks and Resides in the Central Nervous System.” *Cells* 8, no. 10 (October 2019): 1245. https://doi.org/10.3390/cells8101245.

Samarasinghe, Ranmal A., Osvaldo A. Miranda, Jessie E. Buth, Simon Mitchell, Isabella Ferando, Momoko Watanabe, Thomas F. Allison, et al. “Identification of Neural Oscillations and Epileptiform Changes in Human Brain Organoids.” *Nature Neuroscience* 24, no. 10 (October 2021): 1488–1500. https://doi.org/10.1038/s41593-021-00906-5.

Sloan, Steven A., Spyros Darmanis, Nina Huber, Themasap A. Khan, Fikri Birey, Christine Caneda, Richard Reimer, Stephen R. Quake, Ben A. Barres, and Sergiu P. Paşca. “Human Astrocyte Maturation Captured in 3D Cerebral Cortical Spheroids Derived from Pluripotent Stem Cells.” *Neuron* 95, no. 4 (August 2017): 779-790.e6. https://doi.org/10.1016/j.neuron.2017.07.035.

Swain, Susan L., K. Kai McKinstry, and Tara M. Strutt. “Expanding Roles for CD4+ T Cells in Immunity to Viruses.” *Nature Reviews Immunology* 12, no. 2 (February 2012): 136–48. https://doi.org/10.1038/nri3152.

“Volume 32 | HIV Surveillance | Reports | Resource Library | HIV/AIDS | CDC,” May 21, 2021. https://www.cdc.gov/hiv/library/reports/hiv-surveillance/vol-32/index.html.

Wallet, Clementine, Marco De Rovere, Jeanne Van Assche, Fadoua Daouad, Stéphane De Wit, Virginie Gautier, Patrick W. G. Mallon, et al. “Microglial Cells: The Main HIV-1 Reservoir in the Brain.” *Frontiers in Cellular and Infection Microbiology* 9 (2019). https://www.frontiersin.org/article/10.3389/fcimb.2019.00362.

Watanabe, Momoko, Jessie E. Buth, Neda Vishlaghi, Luis de la Torre-Ubieta, Jiannis Taxidis, Baljit S. Khakh, Giovanni Coppola, et al. “Self-Organized Cerebral Organoids with Human-Specific Features Predict Effective Drugs to Combat Zika Virus Infection.” *Cell Reports* 21, no. 2 (October 2017): 517–32. https://doi.org/10.1016/j.celrep.2017.09.047.